ChemComm

COMMUNICATION

View Article Online
View Journal | View Issue

Cite this: *Chem. Commun.*, 2023, **59**, 187

Received 25th October 2022,
Accepted 18th November 2022

DOI: 10.1039/d2cc05786g

rsc.li/chemcomm

Cationic dialanes with fluxional π-bridged cyclopentadienyl ligands†

Philipp Dabringhaus, Silja Zedlitz and Ingo Krossing*

Unique π-cyclopentadienyl bridged dialanes are synthesized as complex salts with aluminate anions by comproportionation of aluminocenium cations $[Al^{III}(Cp)(Cp^*)]^+$/$[Al^{III}Cp_2]^+$ with $[(Al^ICp^*)_4]$. Very short Al–Al bond lengths occur in positively charged Al_2^{4+} fragments. Intriguingly, the prepared asymmetric dialane shows a unique fluxional coordination of the cyclopentadienyl ligands.

The first unsupported dialane was reported already in 1988 by Uhl.[1] Since then, a large variety of dialanes of type $R_2Al–AlR_2$ and their adducts have been prepared, mostly *via* the reduction of the respective aluminium halides with alkali metals.[2] Only recently, anionic ethane-analogous examples $[R_3Al–AlR_3]^{2-}$ were described.[3] In the course of the intense search for and study of aluminylenes and dialumenes, dialanes bridged by alkenes, alkynes, or aromatic hydrocarbons have been prepared.[4,5] This portfolio of bridged dialanes was extended recently by an oxo-bridged anionic dialane with a highly strained Al–Al σ-bond[6] as well as bis-phosphinidene-bridged dialanes.[7] The reversible insertion of aluminylenes into Al–H bonds is a novel pathway to dialanes[8] and allows for the synthesis of the only known cationic dialanes.[9]

Surprisingly, although cyclopentadienyl ligands have been fundamentally important for the development of Al(I) complexes like in the first Al(I) compound $[(AlCp^*)_4]$ ($Cp^* = C_5Me_5$)[10] or in a first Al_4^+ cluster salt,[11] only very few examples of $Al^{II}–Al^{II}$ bound structures stabilized with Cp ligands are known. Complexes of type $[(Al(X)Cp^*)_2]$ (X = Br, I) were reported as intermediates during the reduction of Cp^*AlX_2 complexes to $[(AlCp^*)_4]$.[12] Analogues with the bulkier Cp^{3t}-ligand (Cp^{3t} = 1,3,5-*t*Bu-C_5H_2) are also known.[13] Recently, a bis(aluminocenophane) **I** with a short Al–Al bond was reported (Chart 1).[14] In all of these compounds, either more ionic η^5-coordinated or more covalent η^1-bonded cyclopentadienyl ligands were observed. π-Cp ligands bridging over two metal centres were hitherto reported for very few group 10 metal examples.[15] In the main group, the only known examples comprise π-Cp bridged $M^{II}–M^{II}$ units characterised for M = Ga[16] (**II**) and M = In[17] (**III**).

Here, we report on the syntheses of cationic cyclopentadienyl bridged dialanes *via* comproportionation of Al^ICp^* and aluminocenium cations, which were generated *in situ* by the reduction of Sn(II)/Ge(II) cations or synthesized separately. The starting point for the synthesis of novel cationic dialanes was the reactivity study of Schnöckels $[(AlCp^*)_4]$ towards cyclopentadienylgermanium[18] and -tin[19] cations $[MCp][F\{Al(OR^F)_3\}_2]$ (M = Ge, Sn, $R^F = C(CF_3)_3$), sparked by our discovery of mixed low-valent group 13 complex salts.[20] Reaction of $[MCp]^+$ salts with 0.25 $[(AlCp^*)_4]$ yielded a mixture of various compounds from which single crystals of the asymmetric aluminocenium cation $[Al(Cp)(Cp^*)][F\{Al(OR^F)_3\}_2]$ grew (ESI†). Interestingly, addition of 0.5 equivalents of $[(AlCp^*)_4]$ yielded an elusive π-cyclopentadienyl bridged dialane $[Cp(AlCp^*)_2][F\{Al(OR^F)_3\}_2]$ **1A** as a colourless crystal (eqn (1), ESI†). Reduction of $[MCp]^+$ by $AlCp^*$ was accompanied by Cp abstraction to intermittently form the mixed aluminocenium ion $[Al^{III}(Cp)(Cp^*)]^+$, which probably did undergo comproportionation to **1A** with another Al^ICp^* molecule. This reactivity is surprising, since Al^ICp^* typically forms mixed valent donor–acceptor complexes of type $Cp^*Al \rightarrow AlR_3$ (R = *t*-Bu,[21] C_6F_5[22]) upon reaction with Al^{III}-Lewis acids. Hence, the formation of divalent **1A** would require the presence of the mixed valent Lewis acid–base adduct $[Cp^*Al^I \rightarrow Al^{III}(Cp^*)(Cp)]^+$ **2**. Notably, a

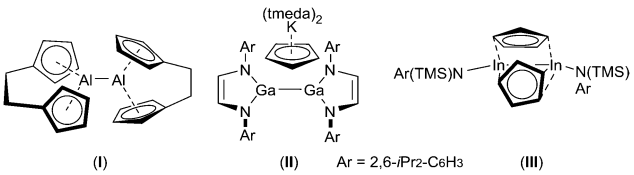

Chart 1 Recently reported aluminocenophane as well as a Cp-bridged digallane and a diindane. TMEDA = tetramethylethylenediamine, TMS = trimethylsilyl.

Albert-Ludwigs University Freiburg, Albertstr. 21, Freiburg 79104, Germany. E-mail: krossing@uni-freiburg.de

† Electronic supplementary information (ESI) available. CCDC 2210630–2210633, and 2214274. For ESI and crystallographic data in CIF or other electronic format see DOI: https://doi.org/10.1039/d2cc05786g

closely related compound has been isolated with [CpGa^{I} → Ga^{III}Cp$_2$I].[23]

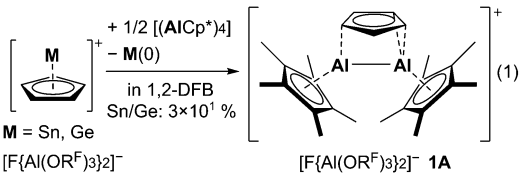

To study this interplay between a mixed-valent Al^{I} → Al^{III} adduct as in **2** and Al^{II}–Al^{II} dialane **1**, we developed a straightforward synthesis of these complexes starting from accessible Al(III) and Al(I) species. We chose the hitherto elusive parent aluminocenium salt [Al^{III}Cp$_2$][Al(OR^F)$_4$] **3** as the starting material. Although the synthesis of [AlCp$_2$]$^+$ was reported in 1996 as an ion pair with a [MeB(C$_6$F$_5$)$_3$]$^-$ counterion[24] and low-temperature NMR analysis clearly confirmed its successful preparation by the characteristic signal at δ^{27}Al = −126.4, no scXRD suitable crystals could be grown. Its structural characterization was achieved in 2009 by switching to a less coordinating anion, *i.e.* [Al(OR^F)$_4$]$^-$ in **3**, prepared by addition of [H(OEt$_2$)$_2$][Al(OR^F)$_4$] to AlCp$_3$.[25] Yet, formation of the ether-adduct [AlCp$_2$(OEt$_2$)$_2$]$^+$ and the instability of solutions of **3** in DCM at temperatures above −20 °C impeded a clean isolation and full characterisation of **3**. Therefore, we developed an easily scalable synthesis of **3** (ESI†). A solution of AlCp$_3$, *in situ* prepared from AlCl$_3$ and MgCp$_2$ in toluene[26] (Scheme 1a), was reacted with [Ph$_3$C][Al(OR^F)$_4$] at room temperature to yield clean **3** as a colourless precipitate in high yield (89%, Scheme 1b).[25] The purity of **3** was verified by NMR spectroscopy in fluorobenzene at room temperature, giving sharp lines at δ^1H = 6.45 and at δ^{27}Al = −130.9. We note that the reduced ion pairing of the cation with the anion [Al(OR^F)$_4$]$^-$ *vs.* [MeB(C$_6$F$_5$)$_3$]$^-$ leads to a pronounced high-field shift by −4.5 ppm. Aluminocenium cation **3** is a potent and accessible Lewis acid (FIA$_{gas}$ = 746, FIA$_{DCM}$ = 241, HIA$_{gas}$ = 716, and HIA$_{DCM}$ = 133)[27] and its reactivity in Lewis acid catalysis or as a cationic Al-source will likely spark future research.

To study the redox reaction between trivalent **3** and Al^{I}Cp*, 0.25 equivalents of [(AlCp*)$_4$] were added to a 1,2-DFB solution of **3** at −40 °C (Scheme 1d). Here, the asymmetric Cp-bridged dialane [Cp(AlCp*)(AlCp)][Al(OR^F)$_4$] **4** was isolated instead of a Lewis acid–base adduct as formulated for **2** (ESI†). Increased addition of 0.5 equivalents [(AlCp*)$_4$] to **3** results in the formation of the [Al(OR^F)$_4$]$^-$ salt of the symmetric dialane [Cp(AlCp*)$_2$]$^+$ **1B**, which is accompanied by the formation of metallic aluminium and hints to the formation of highly labile [(AlCp)$_4$] (ESI†).[28] Moreover, the reaction is accompanied by the formation of the known[28] and rt-stable [CpAl(AlCp*)$_3$] (δ_{AlCp^*} = −76.3, δ_{AlCp} = −108.1). If the parent aluminocenium cation **3** is reacted with 1.25 equiv. [(AlCp*)$_4$], a clean reaction to **1B** and [CpAl(AlCp*)$_3$] is observed and both compounds could be isolated (Scheme 1c, ESI†). Intriguingly, **1B** can also be generated cleanly from **4** by addition of our previously reported low-valent Al$_4$-cluster cation,[11] accompanied by Al(0) precipitation (ESI,† Scheme 1e).

The molecular structures of the symmetric dialanes similarly display short Al–Al bond lengths of 2.518(1) Å in **1A** and 2.508(1) Å in **1B** (Fig. 1), which are only slightly longer compared to the Al–Al bonds in aluminocenophane **I**[14] or highly strained cyclic dialanes.[6,29] Moreover, a similar orientation of the bridging Cp-unit on the Al–Al bond is observed in **1A** and **1B** with distances of 2.297(1) Å and 2.287(1) Å between the Cp-centroids and the midpoint of the Al–Al bond respectively. C–C bond lengths in the bridging Cp ligand differ insignificantly with the shortest bond representing the C2–C3 bond (1.384(4) Å in **1A**, 1.393(3) Å in **1B**) and the longest representing the C1–C2/C3–C4 bonds (1.417(4) Å in **1AB**). The molecular structure of **4** includes four different cations in the asymmetric unit with three different Cp orientations relative to the Al–Al bond. With an average Al–Al bond length of 2.487 Å in **4** (shortest: 2.481(1) Å, $d_{Al-Al,\ range}$ = 2.481(1)–2.492(1) Å), they are even shorter than in the symmetric dialanes **1A** and **1B**. Globally, the only shorter Al–Al bond known to date resides

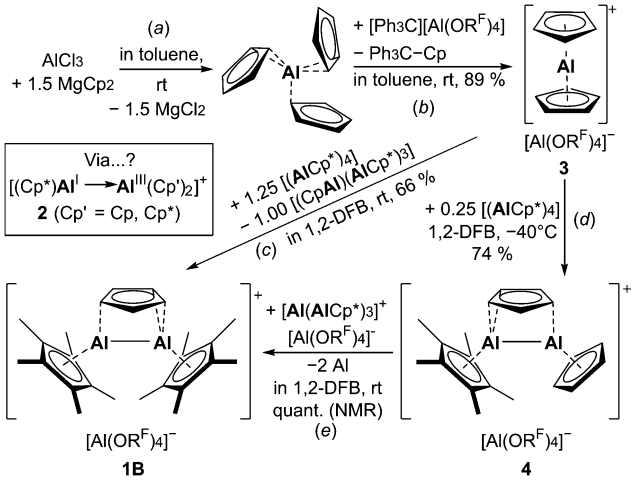

Scheme 1 Synthesis of Cp-bridged dialanes **1B** and **4** *via* the parent aluminocenium cation **3**. 1,2-DFB = 1,2-difluorobenzene; R^F = C(CF$_3$)$_3$.

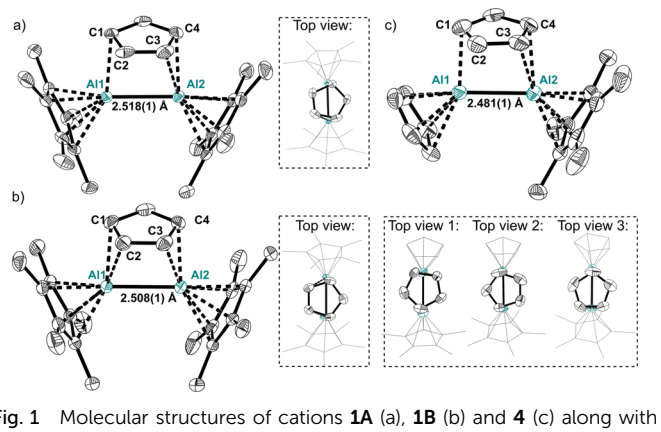

Fig. 1 Molecular structures of cations **1A** (a), **1B** (b) and **4** (c) along with views of different orientations of the bridging Cp ligand. H-atoms and anions are omitted for clarity. Thermal displacement of the ellipsoids is set at 50% probability.

in 1,2-dialuminacyclobutene (2.467(2) Å).[5] Moreover, no considerable changes in C–C bond lengths in the bridging Cp ligands are observed. The flexible coordination of the bridging Cp ligand in **4** is already indicated in the multiple structures detected by scXRD. This flexibility is further confirmed using the ^{1}H NMR spectrum of **4**, where only one singlet is observed at 6.22 ppm for all protons of the inequivalent Cp ligands (ESI†). Hence, not only a rotation of the bridging Cp, but also a rapid exchange between the bridging and the terminal Cp ligands occurs. Moreover, only one broad singlet at δ^{27}Al = −47 is observed for **4** (ESI†). A static structure has computed shifts of the Cp- and Cp*-coordinated aluminium atoms at −63 and −38 ppm respectively. Hence, a complete exchange of the Cp-type ligands in the asymmetric dialane is quick *via* structure **2** rendering all Al atoms and the Cp ligands equivalent on the timescale of NMR. No freezing of the ligand exchange could be observed upon cooling the probe to −40 °C (ESI†). The symmetric dialane displays a broad singlet at δ^{27}Al = −40 (δ_{calc} = −41). These observations are supported by the computed thermodynamics, which reveal an insignificant activation barrier of 0.6/3.2 kJ mol^{-1} for the rotation of the Cp ring in **4**/**1** respectively (Fig. 2). The exchange of the bridging and terminal Cp units in **4** was computed to be a concerted mechanism with a very small activation energy of only 23.2 kJ mol^{-1}. A higher barrier of +44 kJ mol^{-1} was computed for Cp–Cp* exchange (Fig. 2). The transition states of these ligand exchange $\mathbf{TS_I}$ and $\mathbf{TS_{II}}$ resemble the structures expected for classic donor–acceptor Al^{I} → Al^{III} complexes of type **2** (*vide infra*). This fluxional coordination reflects the versatile electronic bonding situation in **4**.

The bonding in dialanes **1** and **4** was further analysed by DFT. Natural bond orbital (NBO) analyses on the Al–Al bonds reveal a σ-bonding interaction with large s character of the Al atoms (>60%) and Wiberg bond orders of 0.99 and 0.96 for the symmetric and asymmetric dialanes respectively (ESI†). The QTAIM analysis (quantum theory of atoms in molecules) yields highly positive charges on the central Al_2 fragment in **4** (Fig. 3a, for **1** see the ESI†). Moreover, a non-nuclear attractor (NNA) resides between the Al atoms in the cations. Similarly to isoelectronic Na_2 and $[Mg–Mg]^{2+}$ fragments,[30,31] NNAs in the formal $[Al–Al]^{4+}$ dimers **1** and **4** originate from significant build-up of electron density upon bonding of Al atoms with high s character[30] and were also calculated for the recently reported aluminocenophane **I**.[14] Due to the NNAs, QTAIM charges of the individual Al atoms cannot be discussed (ESI†). In the EDA-NOCV analysis of **4**, the interaction of the bridged Cp is best described by coordination of a Cp^- anion to the $[CpAl–AlCp^*]^{2+}$ dimer (ESI†). Here, the attractive bonding is dominated by the electrostatic interaction ($\Delta E_{elstat.}$ = −275 kcal mol^{-1} (65%), ΔE_{Orb} = −131 kcal mol^{-1} (31%)). For the alternative fragmentation into $Cp^\bullet$ and $[CpAl–AlCp^*]^{+\bullet}$, the ΔE_{Orb} value is −142 kcal mol^{-1} only slightly higher. Since the ionic fragmentation overestimates ΔE_{elstat}, while the fragmentation into radicals underestimates ΔE_{elstat}, the reality most likely lies between the two extremes. In both fragmentations, the interaction between the σ* orbital of the Al–Al bond and the Cp ligand represents the major orbital interaction (Fig. 3b).

Intrigued by the fluxionality of the ligands in **4**, the computed transition states $\mathbf{TS_I}$ and $\mathbf{TS_{II}}$ were analysed by means of EDA-NOCV and QTAIM (Fig. 3c and d, for $\mathbf{TS_{II}}$ see the ESI†). Similar charges of the central Al_2 fragment are computed for the cations. Contour plots of the Laplacians of $\mathbf{TS_I}$ and $\mathbf{TS_{II}}$ indicate an asymmetry in bonding interaction when compared to **4** (Fig. 3c, ESI†). In the EDA-NOCV analysis, Al–Al bonds in $\mathbf{TS_I}$ and $\mathbf{TS_{II}}$ are best described as covalent bonds by fragmentation into an $[Al(Cp)(Cp/Cp^*)]^\bullet$ and an $[Al(Cp/Cp^*)]^{+\bullet}$ fragment (Fig. 3d, ESI†). Surprisingly, the small eigenvalues of the Δρ plots reveal minor charge accumulation at the η^5-Cp coordinated Al atom. Hence, in contrast to the expected donor–acceptor character in the transition states, $\mathbf{TS_I}$ and $\mathbf{TS_{II}}$ are best described as covalently bound and polarized dialanes.

Finally, the overall thermodynamics for the presented synthetic procedure were computed (Fig. 3e). Exergonic reaction enthalpies are obtained for all observed reaction steps, both in the gas phase and in solution. Moreover, the symmetric dialane **1** is computed to be stable against disproportionation, which is in-line with the experiment. Intriguingly, the disproportionation of the asymmetric dialane **4** into Al^{I}Cp and $[AlCpCp^*]^+$ is more favourable compared to the reformation of $[AlCp_2]^+$ and Al^{I}Cp*. Hence, in principle dialane **4** could function as a stable transfer source of the elusive Al^{I}Cp to a suitable acceptor. Note that solutions of 'Al^{I}Cp' decompose above −60 °C.

In summary, we report cyclopentadienyl bridged, cationic dialanes formed via comproportionation between aluminocenium cations and $[(AlCp^*)_4]$. The asymmetric dialane shows a unique fluxional, ionic coordination of the Cp ligands at the central $[Al–Al]^{4+}$ units. The reactivity of the reported dialanes, combining the electrophilicity of cationic Al species with the reducing ability of dialanes, will be studied in further research.

This work was supported by the Fonds of the Chemical Industry and the DFG (grant KR2046/35-1). Support came from the state of Baden-Württemberg through bwHPC and the DFG

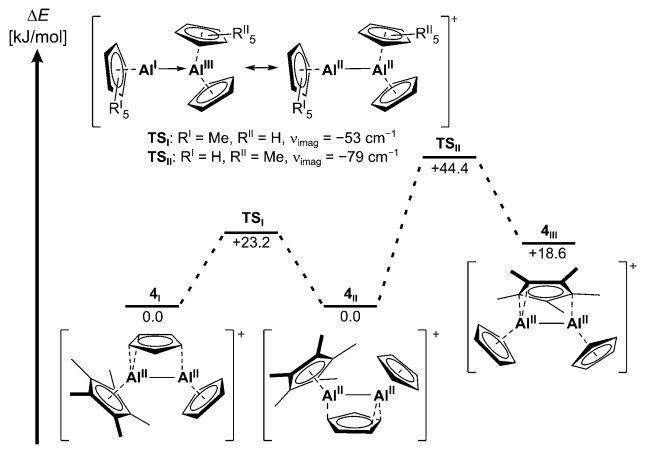

Fig. 2 Reaction profile for exchange of Cp* and Cp ligands in **4** (bp86-d3bj/def2-svp level of DFT). $\mathbf{TS_{I\,and\,II}}$ are not intermediates, but include one imaginary frequency.

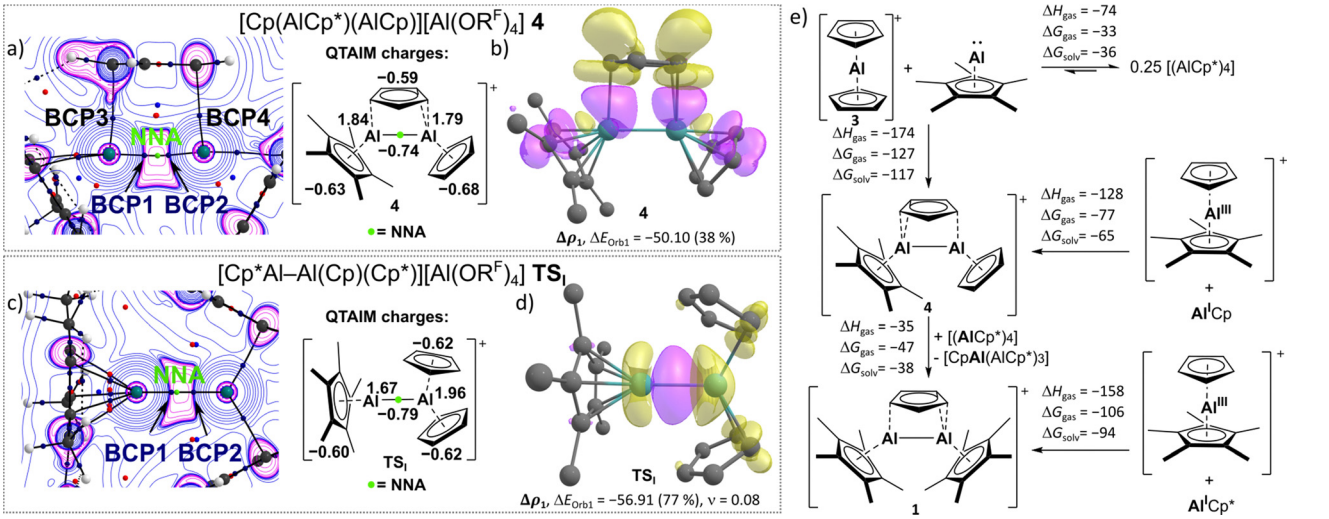

Fig. 3 (a) and (c) Distribution of the Laplacian $\Delta\rho_r$ in the Al–RCP(Cp)–Al planes of **4** (a) and $\mathbf{TS_I}$ (c) with BCP (dark blue), RCP (ring critical point, red) and NNA (green) along with computed QTAIM charges. (b) and (d) Plots of the deformation density $\Delta\rho$ (isovalue 0.001) associated with the major orbital interaction ΔE_{Orb} (values in kcal mol^{-1}) for fragmentation of **4** in $[CpAlAlCp^*]^{2+}$ (singlet) and Cp^- (singlet) (b) and $\mathbf{TS_I}$ in $[AlCp_2]^\bullet$(doublet) and $[AlCp^*]^{+\bullet}$ (doublet) (d) and the eigenvalues ν of $\Delta\rho$. Charge flows from yellow to purple. (e) Gas phase and solution thermodynamics (in 1,2-DFB) for the observed dialane formation as well as their disproportionation into Al(I) and Al(III) species. All values are in kJ mol^{-1}. Computed at the pbe0-d3bj/def2-tzvpp/bp86-d3bj/def2-svp level of DFT, solvation energies with cosmo-rs theory at the bp86-d3bj/def2-svp level.

through grant no INST 40/467-1 and 575-1 FUGG (JUSTUS1/2 cluster).

Conflicts of interest

There are no conflicts to declare.

Notes and references

1 W. Uhl, *Z. Naturforsch. B*, 1988, **43**, 1113.
2 (*a*) Y. Zhao, Y. Liu, L. Yang, J.-G. Yu, S. Li, B. Wu and X.-J. Yang, *Chem. – Eur. J.*, 2012, **18**, 6022; (*b*) K. Koshino and R. Kinjo, *J. Am. Chem. Soc.*, 2020, **142**, 9057; (*c*) S. Kurumada, S. Takamori and M. Yamashita, *Nat. Chem.*, 2020, **12**, 36.
3 (*a*) C. J. Snyder, P. Zavalij, K. Bowen, H. Schnöckel and B. Eichhorn, *Dalton Trans.*, 2015, **44**, 2956; (*b*) S. J. Bonyhady, N. Holzmann, G. Frenking, A. Stasch and C. Jones, *Angew. Chem., Int. Ed.*, 2017, **56**, 8527.
4 (*a*) P. Bag, A. Porzelt, P. J. Altmann and S. Inoue, *J. Am. Chem. Soc.*, 2017, **139**, 14384; (*b*) C. Weetman, A. Porzelt, P. Bag, F. Hanusch and S. Inoue, *Chem. Sci.*, 2020, **11**, 4817; (*c*) R. L. Falconer, K. M. Byrne, G. S. Nichol, T. Krämer and M. J. Cowley, *Angew. Chem., Int. Ed.*, 2021, **60**, 24702.
5 T. Agou, K. Nagata and N. Tokitoh, *Angew. Chem., Int. Ed.*, 2013, **52**, 10818.
6 K. Koshino and R. Kinjo, *J. Am. Chem. Soc.*, 2021, **143**, 18172.
7 S. Nees, F. Fantuzzi, T. Wellnitz, M. Fischer, J.-E. Siewert, J. T. Goettel, A. Hofmann, M. Härterich, H. Braunschweig and C. Hering-Junghans, *Angew. Chem., Int. Ed.*, 2021, **60**, 24318.
8 (*a*) T. Chu, I. Korobkov and G. I. Nikonov, *J. Am. Chem. Soc.*, 2014, **136**, 9195; (*b*) R. L. Falconer, G. S. Nichol, I. V. Smolyar, S. L. Cockroft and M. J. Cowley, *Angew. Chem., Int. Ed.*, 2021, **60**, 2047; (*c*) C. Bakewell, K. Hobson and C. J. Carmalt, *Angew. Chem., Int. Ed.*, 2022, **61**, e202205901.
9 (*a*) L. J. Morris, A. Carpentier, L. Maron and J. Okuda, *Chem. Commun.*, 2021, **57**, 9454; (*b*) J. Kretsch, A. Kreyenschmidt, T. Schillmöller, R. Herbst-Irmer and D. Stalke, *Inorg. Chem.*, 2020, **59**, 13690.
10 C. Dohmeier, C. Robl, M. Tacke and H. Schnöckel, *Angew. Chem., Int. Ed. Engl.*, 1991, **30**, 564.
11 P. Dabringhaus, J. Willrett and I. Krossing, *Nat. Chem.*, 2022, **14**, 1151.
12 S. G. Minasian and J. Arnold, *Chem. Commun.*, 2008, 4043.
13 A. Hofmann, T. Tröster, T. Kupfer and H. Braunschweig, *Chem. Sci.*, 2019, **10**, 3421.
14 W. Haider, D. M. Andrada, I.-A. Bischoff, V. Huch and A. Schäfer, *Dalton Trans.*, 2019, **48**, 14953.
15 (*a*) R. Beck and S. A. Johnson, *Organometallics*, 2013, **32**, 2944; (*b*) H. Werner, A. Kühn, D. J. Tune, C. Krüger, D. J. Brauer, J. C. Sekutowski and Y.-H. Tsay, *Chem. Ber.*, 1977, **110**, 1763; (*c*) G. Hierlmeier, A. Hinz, R. Wolf and J. M. Goicoechea, *Angew. Chem., Int. Ed.*, 2018, **57**, 431.
16 R. J. Baker, C. Jones, M. Kloth and J. A. Platts, *Organometallics*, 2004, **23**, 4811.
17 Z. D. Brown, Z. Zhu, B. D. Ellis and P. P. Power, *Main Group Chem.*, 2010, **9**, 111.
18 M. Schorpp and I. Krossing, *Chem. – Eur. J.*, 2020, **26**, 14109.
19 M. Schleep, C. Hettich, J. Velázquez Rojas, D. Kratzert, T. Ludwig, K. Lieberth and I. Krossing, *Angew. Chem., Int. Ed.*, 2017, **56**, 2880.
20 P. Dabringhaus and I. Krossing, *Chem. Sci.*, 2022, **13**, 12078.
21 S. Schulz, A. Kuczkowski, D. Schuchmann, U. Flörke and M. Nieger, *Organometallics*, 2006, **25**, 5487.
22 J. D. Gorden, C. L. B. Macdonald and A. H. Cowley, *Chem. Commun.*, 2001, 75.
23 C. Schenk, R. Köppe, H. Schnöckel and A. Schnepf, *Eur. J. Inorg. Chem.*, 2011, 3681.
24 M. Bochmann and D. M. Dawson, *Angew. Chem., Int. Ed. Engl.*, 1996, **35**, 2226.
25 M. Huber, A. Kurek, I. Krossing, R. Mülhaupt and H. Schnöckel, *Z. Anorg. Allg. Chem.*, 2009, **635**, 1787.
26 J. D. Fisher, P. H. M. Budzelaar, P. J. Shapiro, R. J. Staples, G. P. A. Yap and A. L. Rheingold, *Organometallics*, 1997, **16**, 871.
27 (*a*) P. Erdmann and L. Greb, *ChemPhysChem*, 2021, **22**, 935; (*b*) Computed on DLPNO-CCSD(T)/aug-cc-pVQZ//PBEh-3c/def2-mSVP level of DFT with CPCM; (*c*) P. Erdmann, J. Leitner, J. Schwarz and L. Greb, *Chem. Phys. Chem.*, 2020, **21**, 987.
28 H. Sitzmann, M. F. Lappert, C. Dohmeier, C. Üffing and H. Schnöckel, *J. Organomet. Chem.*, 1998, **561**, 203.
29 C. Cui, X. Li, C. Wang, J. Zhang, J. Cheng and X. Zhu, *Angew. Chem., Int. Ed.*, 2006, **45**, 2245.
30 J. A. Platts, J. Overgaard, C. Jones, B. B. Iversen and A. Stasch, *J. Phys. Chem. A*, 2011, **115**, 194.
31 (*a*) L.-C. Wu, C. Jones, A. Stasch, J. A. Platts and J. Overgaard, *Eur. J. Inorg. Chem.*, 2014, 5536; (*b*) S. Besnainou, M. Roux and R. Daude, *C. R. Hebd. Seances Acad. Sci.*, 1955, 311; (*c*) J. Cioslowski, *J. Phys. Chem.*, 1990, **94**, 5496.